Auralization of electrical machines in variable operating conditions

M. van der Giet[1], J. Blum[12], P. Dietrich[2], S. Pelzer[2], M. Müller-Trapet[2], M. Pollow[2], M. Vorländer[2] and K. Hameyer[1]

***Abstract*—For the evaluation of the acoustic performance of electrical machines in variable operating conditions, a real-time auralization procedure applicable in virtual reality environments is developed. Electromagnetic forces, structural dynamics and acoustic radiation as well as room acoustic aspects are considered. The combination of electromagnetic simulation with a unit-wave response-based approach and a room acoustic virtual environment software allows for an efficient implementation. Simulation results are shown for two different types of electrical machines—one induction machine and one permanent magnet synchronous machine. Practical experiments are used to fine-tune and validate the numerical models.**

***Index Terms*—Auralization, simulation, acoustic noise, electrical machines, noise and vibration, room acoustics**

I. Introduction

Audible noise emitted from rotating electrical machines becomes more and more problematic. The spectrum of the noise is dominated by tonal components which can be perceived as disturbing single tones. In many applications the annoying sound can devalue the complete drive system. Therefore, it is essential to limit the emitted noise to a tolerable limit. In order to achieve a low-noise design a cost efficient pre-determination of the radiated acoustic noise is important. Therefore, analytical [1] as well as numerical methods [2] can be exploited to pre-determine the sound-field. Results are most commonly the total radiated sound power, describing the electrical machine as a source, or more specific the sound-pressure distribution, e.g. in the free-field. Furthermore, the simulated data is most commonly analyzed in the frequency domain only, e.g. in third-octave bands. If, however, the designer is to evaluate the acoustic performance of an electrical machine under variable operating conditions, the emitted noise, depending on torque and speed, will dynamically change. In this case, it is more sensible to auralize the machine, i.e. to make it audible by creating a sound file from numerical data. A run-up of a machine is only one example of such transient phenomena. As an example for electric cars, this may be a complete standardized drive cycle.

If in addition the acoustic scenario around the machine is to be considered, the acoustic transfer characteristic of the room is required. So far, there are no specific hints of the practical auralization of electrical machines in literature. The simulation of radiated sound, however, is addressed in many papers [1]–[4]. Recent developments have shown the enormous potential of a so called unit-wave response based approach [5], i.e. the structure-dynamic response of a rotating electrical machine to a pure spatially sinusoidal distributed force excitation with an amplitude of unity. Furthermore, room acoustic simulation software and auralization techniques are available [6], [7].

[1]: Institute of Electrical Machines at RWTH Aachen University
[2]: Institute of Technical Acoustics at RWTH Aachen University

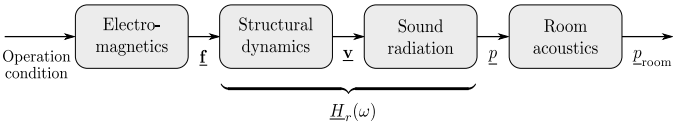

Figure 1. Schematic of transfer function-based auralization concept.

This paper puts together these building blocks and implements a modular completely simulation based procedure for the real-time auralization of electrical machines, following ideas as proposed in [8]. The procedure makes use of the unit-force response approach and is thus both flexible and fast because most of the data can be pre-calculated. Here, two machines, a permanent magnet synchronous machine and an induction machine serve as examples. Measurements and model adaptation are used to fine-tune the structural dynamic and the room acoustic models. The results are evaluated in terms of a run-up and a virtual walkabout in a laboratory hall.

II. Approach

A transfer-function-based approach is developed in this work. Amplitudes of force density waves are directly linked to the free-field sound pressure on an evaluation sphere surrounding the electrical machine. In this way, a division in offline pre-calculation of structural and radiation data and an online-auralization becomes possible. Including a room acoustic simulation including head-related transfer functions, binaural sound signals can be obtained. Employing in addition to the acoustic model an optical model of the room, allows for the immersion into a virtual reality scenario in which the machine is placed.

A. Transfer function concept

As shown in Figure 1, the proposed concept for the real-time auralization of electrical machines consists of four simulation steps: The electromagnetic forces and the structural dynamic behavior are simulated by means of the FEM. The transfer function of the mechanical structure leads to a relation between the electromagnetic force $\underline{\mathbf{f}}$ and the surface velocity $\underline{\mathbf{v}}$. The sound radiation simulation yields the transfer function from surface velocity $\underline{\mathbf{v}}$ to sound pressure $\underline{p}$ at the evaluation points in the free-field. The room acoustic transfer function describes

the sound propagation inside the room from the source to a receiving position.

In the same way as the force-to-velocity transfer function is expanded in a circumferential FOURIER series called *force modes* r, there is also one transfer function from velocity to acoustic pressure per mode. The total transfer function from force to acoustic pressure is thus denoted $\underline{H}_r(\omega)$ for each force mode r. For each observation point and for each mode r, a transfer function from force to acoustic pressure is calculated.

For the room acoustic simulation using RAVEN (Room Acoustics for Virtual Environments, developed at the Institute of Technical Acoustics at RWTH Aachen University for the CAVE-like environment [7]) it is necessary to extract a directivity and a single source signal. The source signal p_{ref} is defined as the sound pressure at one selected observation point. To extract the directivity, the calculated radiation characteristic is normalized. Since the directivity in *RAVEN* is defined in third-octave bands the resulting signals have to be filtered before the directivity can be extracted. The sound signal at the ear is obtained by the convolution of the source signal with the impulse responses for the left ear $h_{\text{l}}(t)$ and the right ear $h_{\text{r}}(t)$

$$\begin{aligned} p_{\text{l}}(t) &= p_{\text{ref}}(t) * h_{\text{l}}(t)\,, \\ p_{\text{r}}(t) &= p_{\text{ref}}(t) * h_{\text{r}}(t)\,. \end{aligned} \tag{1}$$

The source signal given to RAVEN is determined by superposition

$$p_{\text{ref}}(t) = \sum_{r=-R}^{R} \sigma_r(t) * h_r(t) + \sum_{s=-S}^{S} T_s(t) * h_s(t)\,, \tag{2}$$

where $h_r(t)$ is the impulse response of the transfer function $\underline{H}_r(\omega)$ from radial force with mode r to acoustic pressure, and $\underline{H}_s(\omega)$ for the azimuthal case. This approach requires that one directivity can be used for all force modes. If the directivity differs significantly between different force modes, then a directivity per mode has to be determined and superposed in RAVEN. Next, it is shown how the general Equation (2) can be simplified and which basic principles are applied in RAVEN to determine the impulse response of the room.

B. Various operating conditions

Steady-state: If the machine runs at constant speed and all electromagnetic quantities including forces are time-harmonic, then Eq. (2) can be performed beneficially in the frequency domain, since both the transfer function and the force excitations are typically available as spectra. Hence, the source signal is also obtained in the frequency domain

$$\underline{p}_{\text{ref}}(\omega) = \sum_{r=-R}^{R} \underline{\sigma}_r(\omega) \cdot \underline{H}_r(\omega) + \sum_{s=-S}^{S} \underline{T}_s(\omega) \cdot \underline{H}_s(\omega)\,. \tag{3}$$

For auralization an inverse FOURIER transform has to be performed. Since the contributions of the individual force waves are known a-priori, a weighted sum of directivities can be found. Thus, it is possible to only use one directivity per frequency.

Quasi-transient operation of synchronous machines: If the rotational speed of a synchronous machine is time-dependent and the rotor-displacement angle and the current amplitude is time-independent, then forces are time harmonic. In this case, it is possible to modulate the forces by a normalized signal representing the time-dependency of the rotational speed.

For the simulation of a run-up with constant torque linear swept sine signals (sweeps) with an amplitude of unity can be utilized. One sweep for every frequency order μ is used. Besides the force order, the sweep depends on the start speed n_1, the end speed n_2 as well as on the time duration T_{run} of the run-up. The analytic signal of a linear sweep of frequency order μ is defined in time domain by

$$\underline{s}_\mu(t) = \mathrm{e}^{-\mathrm{j}2\pi\mu(n_1 + \frac{n_2 - n_1}{T_{\text{run}}}t)t} \quad 0 \le t \le T_{\text{run}}. \tag{4}$$

These sweeps are convolved with the transfer function. The resulting sound pressure in time domain is calculated as the superposition of all combinations of frequency μ and force order r

$$\begin{aligned} p_{\text{ref}}(t) \quad = \quad & \sum_{\mu=1}^{M} \sum_{r=-R}^{R} \operatorname{Re}\left\{\underline{\sigma}_{r\mu}\underline{s}_\mu(t)\right\} * h_r(t) + \\ & + \sum_{\mu=1}^{M} \sum_{s=-S}^{S} \operatorname{Re}\left\{\underline{T}_{s\mu}\underline{s}_\mu(t)\right\} * h_s(t) \end{aligned} \tag{5}$$

C. Radiation and Cylinder

The sound-radiation transfer-function can be computed by means of the boundary element method (BEM) or an analytical model. In most practical applications of rotating electrical machines, the housing of the machine can be approximated by a cylinder. Therefore, an analytical model based on the solution of the HELMHOLTZ equation in cylindrical coordinates has been derived following the approach of harmonic decomposition [9] and tested for practical electrical machines [10].

The model describes an infinite cylindrical radiator with a finite-length surface velocity distribution. Thus, end-effects can be taken into account. Compared to the BEM, the analytical cylinder model is approx. 2000 times faster, depending on the frequency. Even if the shape of the machine is not a perfect cylinder, the analytical model showed a good accuracy compared to the BEM and is, hence, preferred here [10].

D. Room acoustic simulation and acoustic virtual reality

The sound perceived at a given point in a room is determined by the sound source and receiver position on the one hand and by the properties of the room on the other hand. The source is in this case an electrical machine and the room may for example be a factory hall. For frequencies above the so-called SCHROEDER frequency geometrical acoustics can be used. This frequency limit is approximated by

$$f_{\text{s}} \approx 1200\,\text{Hz} \cdot \sqrt{\frac{T_{\text{rev}}/\text{s}}{V/\text{m}^3}}, \tag{6}$$

where V is the volume of the room and T_{rev} is the reverberation time. The reverberation time is defined as a time span that passes by until the energy density in a stationary excited room drops by $60\,\text{dB}$ after the sound source has been suddenly switched off.

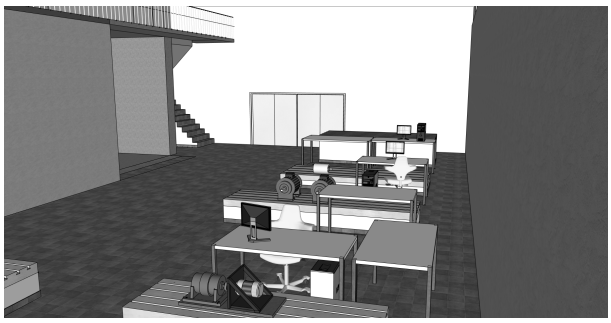

Figure 2. IEM laboratory hall—optical model for virtual reality.

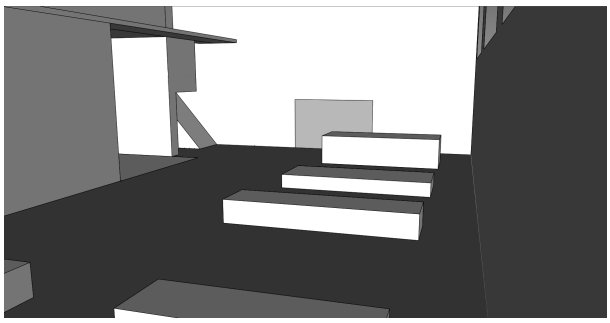

Figure 3. IEM laboratory hall—acoustical model for virtual reality.

In geometric acoustics, sound is represented by sound rays which are thin lines of sound particles which transport acoustic energy though they do not show typical wave effects, such as diffraction and interference. Basically two different principles are used and are often combined in simulations that are based on geometric acoustics [6]. They are referred to as image sources and stochastic ray tracing. Both methods are combined in the room acoustic software *RAVEN* used in this work.

Room model: Rooms usually contain lots of details, e.g. stairs, lamps, furniture or, in case of a laboratory hall, other machines, racks and further technical equipment. These details however should not be taken into account in the acoustic room. On the one hand, this is because they would increase the computational effort without adding significant audible information, on the other hand, it may even induce additional error because the fundamental assumptions of geometrical acoustics are violated. Therefore, details that are not large compared to the wavelength are not considered in the model. The remaining flat surfaces are modeled with adjusted absorption and scattering parameters. In most cases, a resolution of objects and faces of approximately 0.5 m is appropriate (as proposed in [11]).

In order to immerge into the virtual scenario, the acoustic perception has to be accompanied by an appropriate visual impression. Therefore, next to the acoustic model, a visual representation is to be created. As the optical model is not used for simulation but only for visual feed-back, it can be rich in detail. A 3D representation of one laboratory hall of the IEM is created using the software *Google SketchUp*. The acoustic model is deduced from the optical model and imported into RAVEN. Figures 2 and 3 show these two models. Three different materials are defined in the acoustic model, for walls, the floor and windows. Since the reverberation time of a room is important for the acoustic impression, absorption and scattering coefficients of the three materials are adjusted to meet the measured reverberation time of approx. 2.25 s.

E. Mechanical and aerodynamic noise

The noise radiated by an electrical machine has more components than those originating from magnetic forces. To make the impression of the auralized machine noise sound more realistic, i.e. less synthetic, broad band noise components are added that account for mechanical and aerodynamic components. Noise is modulated with the frequency of rotation which drastically improves the authenticity. The strength of the additional noise components increases with the speed of the machine. Good results are obtained for additional noise in the frequency range from 300 Hz to 1.3 kHz and a modulation factor of 0.2. . .0.4.

Table I
GEOMETRICAL DATA OF THE SYNCHRONOUS MACHINE.

Parameter	Symbol	Value
Number of stator slots	N_1	6
Number of magnets	$2p$	4
Stator outer Diameter	D_o	300 mm
Stator inner Diameter	D_i	170 mm
Air gap	δ	1 mm
Height of yoke	h_y	28 mm
Height of magnets	h_m	10 mm
Width of the slot opening	b_N	$\frac{2\pi}{15}$ rad
Active length	l_z	400 mm

III. RESULTS

A. Example: Run-up of a synchronous machine

A PM synchronous machine is used as a first example: The stator consists of a laminated sheet stack (M250-AP) with slots and the rotor is made from the same material and is equipped with surface-mounted permanent magnets ($\mu_\mathrm{r} \approx 1$, $B_\mathrm{rem} = 1.17\,\mathrm{T}$). The geometrical parameters are given in Table I. The number of stator slots is $N_1 = 6$ and the number of magnets is $2p = 4$.

1) Transfer function: The transfer functions relating force densities to sound pressure are calculated. The resulting sound pressure distributions per unit-force are shown in Figure 4. It can be seen that even force orders cause a rotating velocity distribution where the radiation pattern of force order 3 indicates standing velocity distributions almost independent of the frequency. Figure 5 shows the results of the unit-wave response-based approach: the sound power radiated by each force mode r.

2) Run-up simulation: In order to simulate a run-up, sweep signals according to Eq. 4 are generated up to an order of 100. Thereby, the length of the signal is set to 5 s, start and end speed are chosen to be 600 and 6000 min^{-1}. After the multiplication with the actual electromagnetic force density amplitudes, the resulting sound pressure signal is obtained in 5 m distance. It is presented in form of a spectrogram shown in Figure 6.

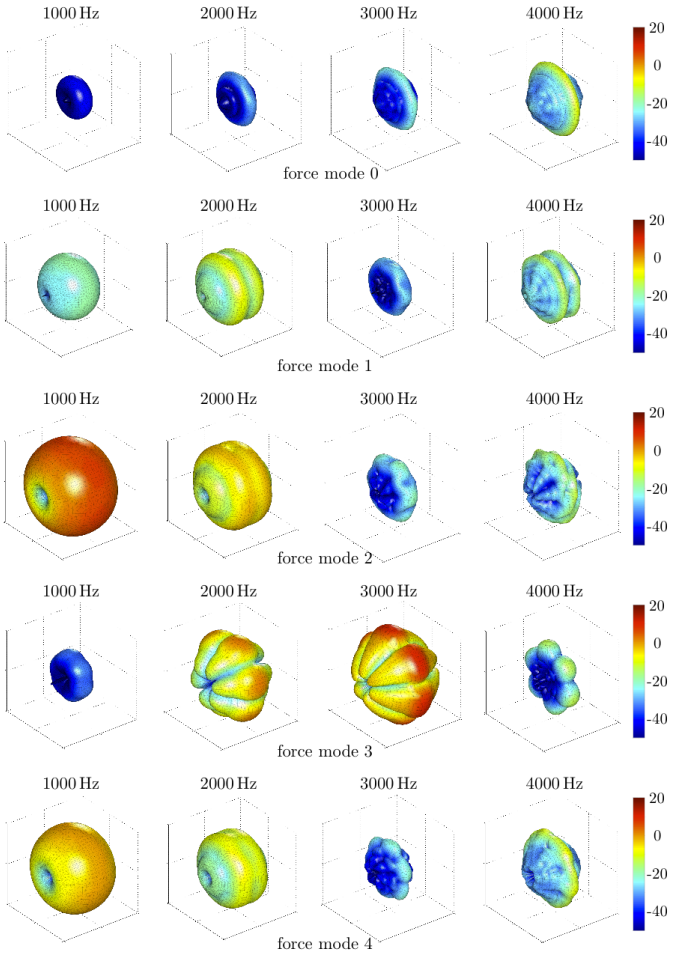

Figure 4. Sound-pressure level per unit-force in (dB re 20 μPa/Pa) for radial force modes 0 . . . 4.

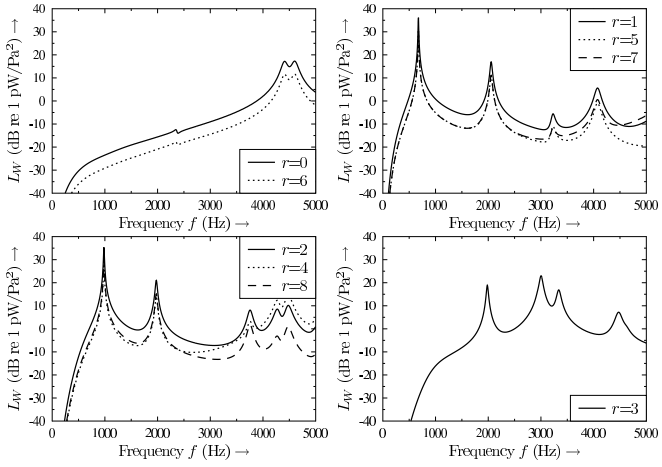

Figure 5. Sound-power level per unit-force.

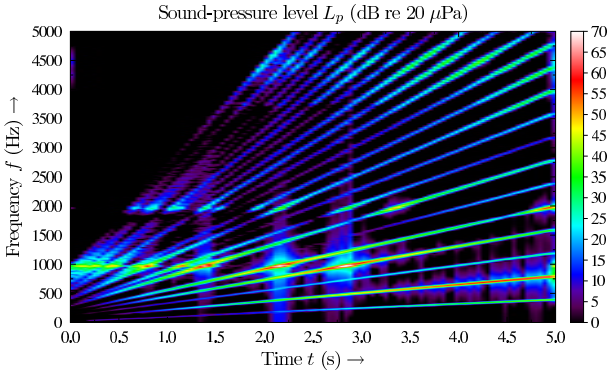

Figure 6. Spectrum of a simulated run-up from 600 to 6000 min^{-1}.

Table II
SPECIFICATIONS OF THE INDUCTION MACHINE UNDER INVESTIGATION.

Power rating:	750 W	q:	3	Inner stator radius:	35 mm
Poles:	$2p = 4$	Winding scheme:	1/8/10/12	Outer stator radius:	60 mm
Stator slots:	36	Rotor skewing:	15 °	Active length:	80 mm
Rotor slots:	28	Mass:	7.880 kg	Total length:	160 mm

In the vicinity of certain eigenfrequencies of structural modes that are likely to be excited, the sound pressure increases significantly. In particular, those natural frequencies are located around 1 kHz, 2 kHz and 4.5 kHz.

In Figure 6, several order lines are visible. Each line is excited by a certain time-harmonic order μ, which is determined by the slope in the spectrogram, and by multiple of space orders r. Despite this superposition of different space orders, one time harmonic order line is most commonly dominated by a single force space order.

B. Example: Induction machine in a virtual factory hall

A new factory hall is planned with different types of machinery. Significant sources of acoustic noise are the electrical machines. To reduce the overall noise level in the hall for worker protection, a room acoustic simulation model is derived that describes the electromagnetic noise with the flexibility to account for different load and operation conditions such as a run-up. In addition, the machines should be relocatable in the room such that in a subsequent step, it can be assessed how to use sound suppression measures most effectively for this scenario. Since this work is concerned with the vibro-acoustic characteristic of electrical machines, the latter aspect is out of the scope of this paper. It is focused here on the technical realization and validation of the simulation chain only. A small induction machine designed for continuous run and grid supply is used as an example because induction machines are the most commonly used machine type in industry for their comparatively simple design, rugged configuration and versatility. The machine under investigation is a $2p = 4$-pole three-phase squirrel cage induction machine described by the specifications in Table II.

The model geometry can be seen in Figure 7. It contains the stator, stator winding, winding overhang, the rotor with shaft and the end-bells. Each of these components is modeled with specific material properties that are explained in more detail in the next section. Bearings are modeled as simple rings with

Figure 7. Structure dynamic model of the induction machine.

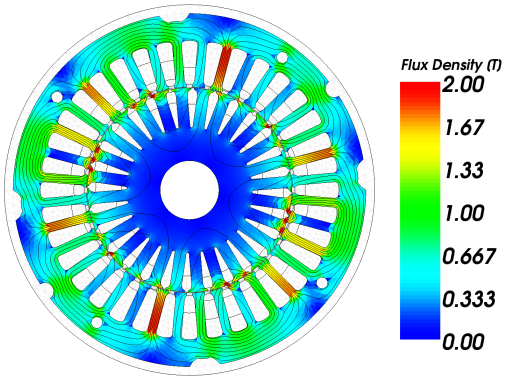

Figure 8. Magnetic flux density distribution and magnetic field lines.

a stiff connection to the shaft. Since the drive-end end-bell is mounted to a relatively rigid construction, displacements of the nodes connected to the construction are set to zero for the modal analysis.

1) Transfer function: The transfer function from forces to surface velocity and from surface velocity to free-field sound pressure is established by a modal superposition of unit forces [5] and by the analytical cylinder model, respectively.

The velocity per unit-force is used as excitation to determine a relation from force densities to sound pressure at the observation points. Rotating forces lead to a rotating velocity distribution. Therefore, the radiation pattern cannot be interpreted as a snap-shot but more as a timely average.

Due to the imperfect symmetric shape and due to the stator teeth the forces act on, every force mode excites every structural mode, even though the intensity of the excitation varies significantly. A force mode of order r is likely to excite a structural mode of order $n = r$ the most, however, significant contributions can stem from other modes. When the corresponding structural natural frequency is for example far above the frequency of the force, structural response can even be dominated by a mode $n \neq r$. In this case, radiation patterns are closer to that of a cylinder vibrating with the structural order, i.e. n. With the exception of the so-called breathing mode 0, modes of higher order usually occur at higher frequencies. Here mode 2 has natural frequencies of approximately $1.5\,\mathrm{kHz}$ while those of order 4 are approximately $6\,\mathrm{kHz}$. For this reason, the explained effect is more prevalent for force modes of higher order. Particularly force modes $5 \ldots 8$ show this effect. Although forces rotate, in this case, the resulting velocity does not. This effect stems from the rotational speed of the force wave. If the force order is higher than that of the excited structural mode, forces rotate slower than the structural mode allows.

2) Electromagnetic excitation: In order to use the transfer function, the force densities during operation of the induction machine are to be calculated. The electromagnetic field problem is solved using the FEM with eddy current allowed in the rotor bars. When steady-state conditions are reached the mean torque is approximately $3.49\,\mathrm{Nm}$. The flux density distribution of one time step can be seen in Figure 8. Skewing is accounted for by means of the multi-slice method [12]. Electromagnetic force-density waves are extracted as nodal forces.

3) Experimental verification: To validate the results of the three simulation tasks, i.e. electromagnetic, structural dynamic and acoustic simulation, different measurements are performed. Since it is a difficult task to measure the magnetic field or radial forces, the electromagnetic simulation is only verified by measuring torque. This point of operation is given by: $V = 400\,\mathrm{V}$, $f_1 = 50\,\mathrm{Hz}$, $n = 1380\,1/\mathrm{min}$, $s = 8\,\%$, $I_1 = 1.65\,\mathrm{A}$, and $T = 3.37\,\mathrm{Nm}$. Results from the structural dynamic analysis are validated by measuring the velocity on the outer surface of the machine using a laser vibro-meter.

Basically, two different measurement setups are used: one for the determination of the sound power and the surface velocity and the other one for the measurement of the radiated sound pressure. In both cases the machine is mounted on a testbed and connected to a powder break because it is comparatively quiet. Voltage and current of the induction machine are measured, using common power meters in ARON-configuration. All measurements are performed using the *ITA-Toolbox* in *MATLAB*.

The measured torque is $3.37\,\mathrm{Nm}$, the mean simulated torque is $3.49\,\mathrm{Nm}$, resulting in a relative error of approximately $3.5\,\%$. Sound power determination is done using a reverberation chamber under consideration of the standard *ISO 3743-2*. The comparison between measured and simulated sound-power levels in third-octave bands is shown in Figure 9. The sound power level at lower frequencies is underestimated while the prediction for higher frequencies is above the measured values. Even though the simulated velocity at $744\,\mathrm{Hz}$ almost perfectly matches the measured one, the sound power in the corresponding band shows differences of approximately $30\,\mathrm{dB}$. One possible reason for this can be additional noise stemming from bearings, the break and other structural vibrations caused by the connection between the two machines or the background noise of the room. Another reason for the underestimation of the sound power at low frequencies could be the fact that influences of the mounting are neglected within the simulation procedure. Especially at lower frequencies the radiation of the small cylinder itself is very inefficient, leading to a low radiated sound power. The additional surface of the mounting can significantly increase radiated noise. For this reason the influence of the mounting is analyzed by means of BEM and it is found that a major part of the additional measured noise stems from the mounting.

4) Auralization in a virtual factory hall: To demonstrate the auralization procedure, the IEM machinery hall is used as an example. Therefore, the continuously running induction machine is placed on a machine foundation. A path through

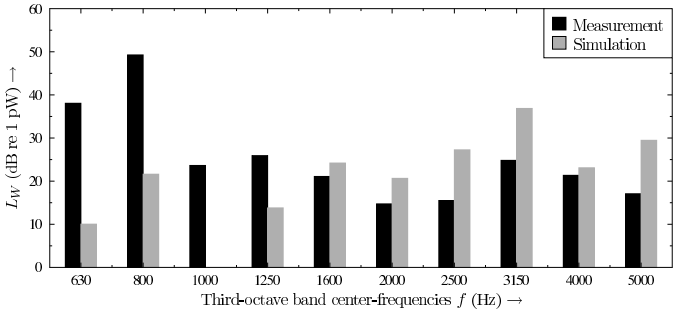

Figure 9. Comparison of measured and simulated sound-power levels in third-octave bands.

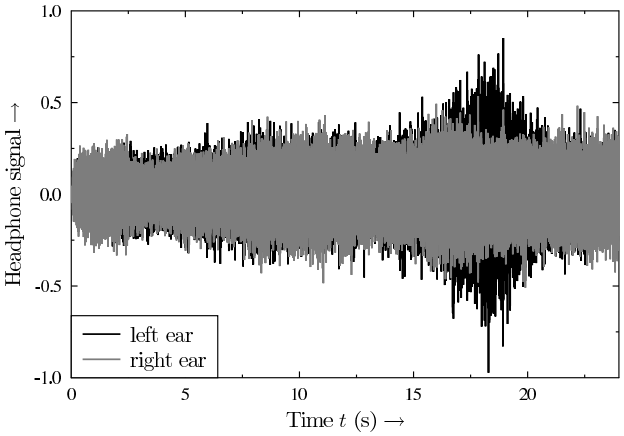

Figure 10. Time history of headphone signals during a virtual walkabout (normalized).

the virtual hall is defined starting from the first floor, down the stairs, around to the back of the hall and heading towards the machine. After that the machine is left behind and the path leads to the exit. The walking speed is adjusted so that the whole walk takes 25 s. The binaural signal is recorded from the RAVEN simulation and its time history is shown in Figure 10. The computation took in total approx. 1.5 h on a standard dual-core computer. With a reduced quality and parallelization of the time consuming convolution, it is possible to perform the required computation in real-time. It can be seen that due to turns and different sound fields reaching the left and the right ear, e.g. by shadows of walls etc., the signals of the left and the right ear are different.

To further visualize the acoustic-walkabout, a short-time DFT of the recorded signal is performed resulting in the spectrogram shown in Figure 11. As the machine is running at constant speed, the spectrogram is dominated by horizontal lines. It can be seen that the tonal noise stemming from the induction machine gives rise to thin spectral lines above approx. 2 kHz. Three broad-band signals are visible around 1 kHz. This is noise added by means of the noise mode, presented in Section II-E. The point during the walkabout closest to the machine, approx. 17 s, is clearly visible by the high levels.

IV. Summary and Conclusions

The combination of electromagnetic simulation with a unit-wave response-based approach and a room acoustic virtual

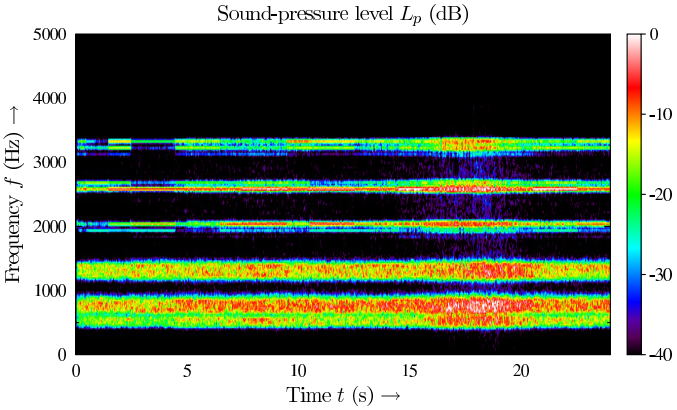

Figure 11. Spectrogram of the sound pressure at the left ear during a virtual walkabout in a factory hall (normalized).

environment software allows for an efficient implementation of a procedure for the real-time simulation- based auralization of rotating electrical machines. It is shown how the modular approach can be used for different machines and different questions regarding the operation condition. The general case of dynamic change of speed and torque requires an online calculation of the electromagnetic force excitations where only one force calculation is necessary for the run-up of a synchronous machine at constant torque.

References

[1] H. Jordan, *Geräuscharme Elektromotoren*. W. Girardet, November 1950.

[2] C. Wang, J. Lai, and A. Astfalck, "Sound power radiated from an inverter driven induction motor II: Numerical analysis," *IEE Proceedings Electric Power Applications*, vol. 151, pp. 341–348, May 2004.

[3] Z. Zhu and D. Howe, "Improved methods for prediction of electromagnetic noise radiated by electrical machines," *IEE Proceedings - Electric Power Applications*, vol. 141, no. 2, pp. 109–120, 1994.

[4] C. Wang and J. Lai, "Sound power radiated from an inverter-driven induction motor. part III: statistical energy analysis," *IEE Proceedings Electric Power Applications*, vol. 152, pp. 619–626, May 2005.

[5] J. Roivainen, "Unit-wave response-based modeling of electromechanical noise and vibration of electrical machines," Ph.D. dissertation, Helsinki University of Technology, 2009.

[6] M. Vorländer, *Auralization - Fundamentals of acoustics, modelling, simulation, algorithms and acoustic virtual reality*, RWTH edition ed. Springer-Verlag Berlin Heidelberg, 2008.

[7] T. Lentz, D. Schröder, M. Vorländer, and I. Assenmacher, "Virtual reality system with integrated sound field simulation and reproduction," *EURASIP Journal on Advances in Signal Processing*, vol. 2007, pp. 1–19, 2007.

[8] S. Fingerhuth, P. Dietrich, M. Pollow, M. Vorländer, D. Franck, M. van der Giet, K. Hameyer, M. Bösing, K. A. Kasper, and R. W. D. Doncker, "Towards the auralization of electrical machines in complex virtual scenarios," in *40th Congreso Nacional de Acústica, TECNIACUSTICA*, Cadiz, Spain, September 2009.

[9] E. G. Williams, *Fourier acoustics: Sound radiation and nearfield acoustical holography*. Academic Press, 1999.

[10] M. van der Giet, M. Müller-Trapet, P. Dietrich, M. Pollow, J. Blum, K. Hameyer, and M. Vorländer, "Comparison of acoustic single-value parameters for the design process of electrical machines," in *39th International Congress on Noise Control Engineering INTER-NOISE*, Lisbon, Portugal, June 2010.

[11] S. Pelzer and M. Vorländer, "Frequency- and time-dependent geometry for real-time auralizations," in *Proceedings of 20th International Congress on Acoustics, ICA 2010*, Sydney, Australia, August 2010.

[12] J. Gyselinck, L. Vandevelde, and J. Melkebeek, "Multi-slice FE modeling of electrical machines with skewed slots-the skew discretization error," *IEEE Transactions on Magnetics*, vol. 37, no. 5, pp. 3233–3237, 2001.